Capacitive Sensing of Interfacial Stresses

Kishore Sundara-Rajan[1], Aaron Bestick[1], Gabriel I. Rowe[1], Glenn K. Klute[2], William R. Ledoux[2], and Alexander V. Mamishev[1]

[1]Sensors, Energy, and Automation Laboratory
Department of Electrical Engineering
University of Washington
Seattle, USA
kishore@u.washington.edu

[2]Center of Excellence for Limb Loss Prevention and Prosthetic Engineering
VA Puget Sound Health Care System
Seattle, USA

***Abstract*—Studying interfacial stresses is an important step towards understanding load distributions in mechanical, biomedical, and industrial systems. This paper presents a capacitive sensor that is capable of simultaneously measuring compressive and shear stresses. The sensor consists of two electrode layers separated by a set of flexible and compressible polymer pillars. The sensor's response to compressive and shear stresses was tested and characterized up to 320 kPa and 70 kPa respectively. An algorithm to estimate the applied stresses based on sensor output was developed and validated. The applied compressive stresses were estimated with an accuracy of 95.04 % and shear stress with an accuracy of 89.45 %.**

I. INTRODUCTION

In the United States, 623,000 civilians live with a lower limb amputation [1]. A large proportion of these lower-limb amputees use prosthetic limbs for mobility, yet their performance is greatly inferior to that of natural limbs. Achieving patient comfort without sacrificing mobility is the primary concern for amputees undergoing rehabilitation after amputation. Comfort and mobility are influenced by the fit of the prosthetic socket system [2,3] and load distribution (normal and shear stress) from the socket to the residual limb. To help improve patient comfort, numerous studies have been conducted recently to understand the implied but complex relationship between pressure, shear stress, fit, and injury. Many investigators have attempted to understand load transfer between the residual limb and the prosthetic socket by studying: a) the direct measurement of interface stress [4,5] at specific limb locations [6]; b) the effect of varying socket types [7,8]; c) the suspension systems [9,10]; d) the amount of interface friction [11]; and e) the variation over time [12]. The interfacial stress sensor discussed in this paper will help improve the understanding of these complex relationships by providing doctors a tool to measure interfacial stress with high accuracy.

The sensor presented here is a continuation of the work presented in [13,14]. The work presented in [13] shows the viability of using capacitive sensors for measuring interfacial forces, and [14] discusses the electrical and mechanical characteristics of the sensor in detail. The work presented in this paper details the inverse problem wherein a model is developed to estimate the applied compressive and shear stresses based on the measured capacitances.

The existing devices for transduction of shear and pressure forces include resistive strain gauges [15], piezoelectric resistors [16], fiber-optic cables and waveguides [17], gas-filled cavities [18], and capacitance-based methods [19-22]. They are all either incapable of simultaneously measuring both forms of stresses, or lack adequate resolution. Furthermore, the range and sensitivity of the existing sensors cannot be easily tuned to suite the application of interest, thereby making them sub-optimal solutions. For example, when studying interfacial forces between the prosthesis and residual limb, the region at the bottom of the limb will experience higher compressive stress than shear, while the regions along the sides of the limb will experience higher shear stresses than compressive stress. If the same sensor is used to measure forces at both of these regions, it will have sub-optimal pressure performance in the bottom region, and sub-optimal shear performance along the sides. In the sensor presented in this paper, the stress-strain relationship can be easily tuned for optimal performance in the expected range of stresses by altering the physical dimensions of the pillar. This flexibility allows researchers to gather higher accuracy data in all regions without having to use complex multi-modal sensing instrumentation.

The shear sensor is a simple parallel plate capacitance sensor, with two electrode layers separated by flexible and compressible pillars made of polydimethylsiloxane (PDMS, Fig. 1).

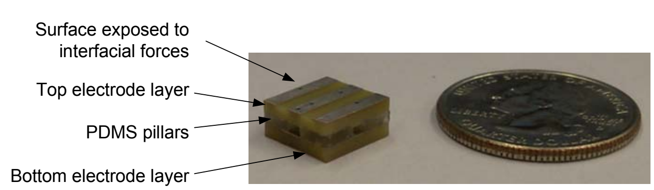

Figure 1. Photograph of the interfacial stress sensor.

This work was supported in part by the U.S. National Institute of Health under Grant R21HD052109-02, the Department of Veterans Affairs Grant A4843C, and the Washington NASA Space Grant scholarships.

Fig. 2a shows the electrode configuration of the sensor. The sensing unit has four electrodes, comprised of one drive electrode and three sense electrodes: 1) the pressure sensor, 2) X-directional shear, and 3) Y-directional shear. When a normal force is applied, the pillars compress, and the distance between the electrodes is reduced, thereby increasing the capacitance between the drive electrode and all the sensing electrodes. When a shear stress is applied, the pillars bend, and the areas of overlap between the electrode layers are changed (Fig. 2b). The electrodes are laid out such that the pressure sensing electrode has significant overlap with the drive electrode and its output is, therefore, immune to lateral displacements. The shear sensing electrodes are designed such that they are sensitive to change in areas of overlap along only one direction, and therefore their outputs are immune to crosstalk.

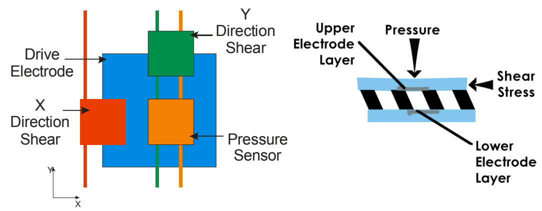

(a) (b)

Figure 2. Simplified electrode configuration of interfacial force sensor.

II. Sensor Characterization

To determine the transfer function of the sensor, it was tested using the Mach-1 micromechanical testing system (BioMomentum Inc., Canada) with a six-axis load cell (Nano17; ATI Industrial Automation). A charge integration based circuit, with a resolution of 4pF, was used to measure the output capacitances. The circuit uses an average of 100 successive samples to mitigate errors due to white noise. The sensor cell was subjected to a range of compressive stresses (up to 320 kPa), and at each compressive stress level, was subjected to shear stresses (up to 70 kPa). The trans-capacitance of the pressure and shear sensing electrodes were measured at each stress level (Fig. 3 and Fig. 4, respectively).

III. Data Analysis

The output capacitance of the pressure sensing electrode varied linearly with the applied compressive stress (Fig. 3), and was insensitive to shear stresses. The expected relationship would be an asymptotic one since the capacitance between a set of parallel plate electrodes varies inversely with the distance between them. Since PDMS is a hyper-elastic material, its stress-strain relationship is non-linear. In the range of forces the sensor was tested in, the non-linearties introduced by capacitance-strain and stress-strain relationships cancel each other, thereby resulting in a linear stress-capacitance dependency. The exact nature of the stress-strain and capacitance-strain relationships can be found in [14]. The relationship between applied compressive stress and capacitance of pressure sensor is given by,

$$C_P = 0.7811\sigma_C + 6.1166 \quad (1)$$

where, C_p is the measured capacitance of the pressure sensing electrode, and σ_C is the applied compressive stress.

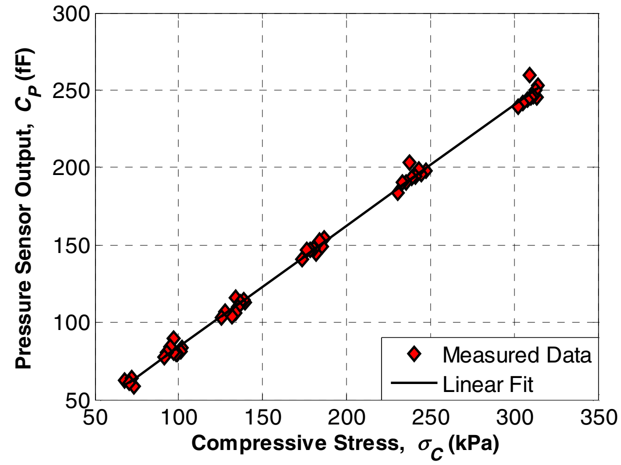

Figure 3. Output of pressure sensor varies linearly with the applied stress.

Since the shear sensing electrodes are rectangular in shape and placed such that their area of overlap with the drive electrode can vary due to lateral displacements along only one direction, their output capacitances vary linearly with applied shear stresses (Fig. 4). The distance between the shear sensing electrodes and the drive electrode is a function of the compressive stress, and is reflected as capacitance offsets between the curves in Fig. 4 at zero shear stress. The relationship between the capacitance of the shear sensing electrode, C_S, and shear stress, σ_S , can therefore be described by the equation,

$$C_S = C_{SB} + m_s\sigma_S \quad (2)$$

where C_{SB} is the baseline capacitance of the shear sensor, defined as its output at zero shear stress, and m_s is the sensitivity of the sensor.

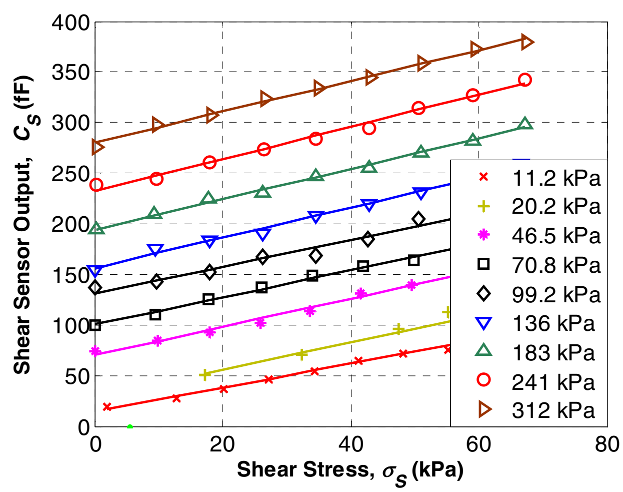

Figure 4. Output of shear sensor varies linearly with the applied stress and is dependent on compressive stress.

The relationship between the change in baseline capacitances of shear sensing electrodes (ΔC_{SB}) and compressive stress is non-linear (Fig. 5) and can be approximated to a quadratic fit given by,

$$\Delta C_{Sb} = -5.078\sigma_C^2 \times 10^{-4} + 0.374\sigma_C \qquad (3)$$

While both the changes in capacitance of the pressure sensor (C_p) and the baseline capacitance of the shear sensor (ΔC_{SB}) are dependent on the compressive stress and are effects of change in the distance between the sense and drive electrodes, the change in C_P is linear, and ΔC_{SB} is non-linear. This inconsistency is due to the non-linearity introduced by fringing field interactions between the shear sensing electrode and the drive electrode. As the sense electrodes move closer to the drive electrode the number of fringing fields that couple the electrode pair increases. In the case of the pressure sensing electrode, since it always has a significant area of overlap with the drive electrode, the number of fringing field lines coupling the pressure sensing electrode and the drive electrode are nearly constant irrespective of the distance between the electrode pairs.

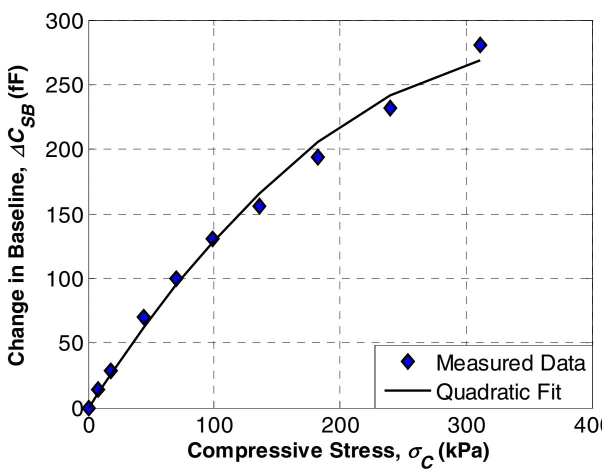

Figure 5. The relationship between baseline capacitance of shear sensor and compressive stress is non-linear and can be approximated to a quadratic fit.

The dependence of fringing field interaction between the shear sensing electrode and drive electrode on compressive stress also affects the sensitivity of the shear sensor, and is reflected as the variation of the slope of the shear sensor output (Fig. 6). This asymptotic non-linear relationship can be modeled as,

$$m_s = 2.216\sigma_C^{-0.386} + 2.324 \qquad (4)$$

IV. Stress Estimation and Validation

To goal of the work presented in this paper is to estimate the applied stresses based on the measured capacitances C_P and C_S.

To estimate the compressive stress, we use linear and one-to-one mapping between the pressure sensor capacitance and compressive stress. The compressive stress estimate, $\tilde{\sigma}_C$, can be obtained by algebraic manipulation of (1), and is given by,

$$\tilde{\sigma}_C = 4.816C_P + 7.538 \qquad (5)$$

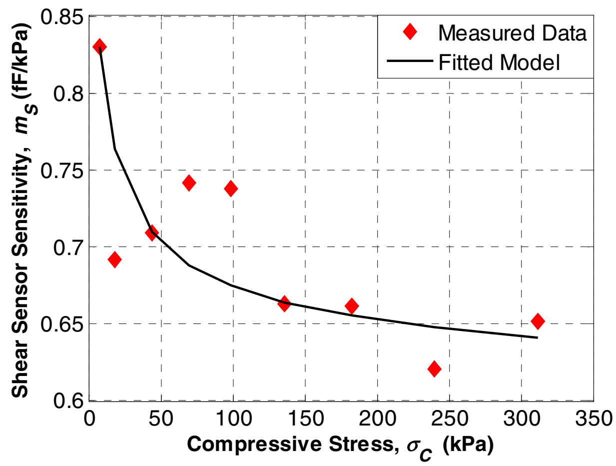

Figure 6. Relationship between the slope of the shear sensor output and compressive stress.

The shear stress estimate, $\tilde{\sigma}_S$, can be obtained from algebraic manipulation of (2). The estimates for shear sensor baseline, $\tilde{C}_{SB}$, and sensitivity, $\tilde{m}_S$, are obtained from (3) and (4) based on the estimated compressive stress, $\tilde{\sigma}_C$. The estimated shear stress is given by,

$$\tilde{\sigma}_S = \frac{C_S - 0.374\tilde{\sigma}_C + 5.078\times10^{-4}\tilde{\sigma}_C^2}{2.216\tilde{\sigma}_C^{-0.386} + 2.324} \qquad (6)$$

The stress estimation process described by (5) and (6) can be validated by comparing the stress estimates predicted by these equations against the known true values of the stresses (Fig. 7 and Fig. 8).

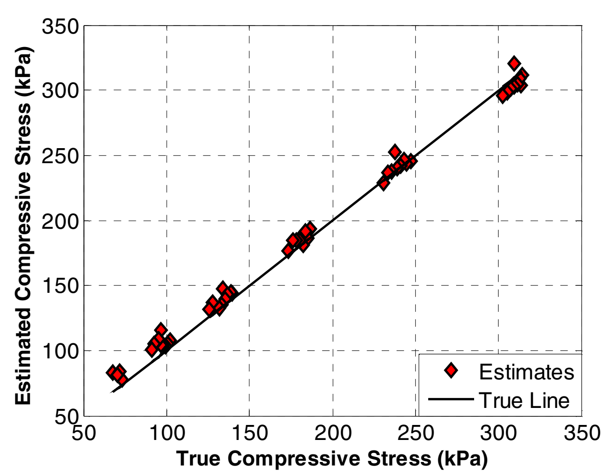

Figure 7. Compressive stress can be estimated with an average accuracy of 95.04 %.

For the data set presented in this paper, the compressive and shear stresses were estimated from the sensor output with an accuracy of 95.04 %, and 89.45 %, respectively.

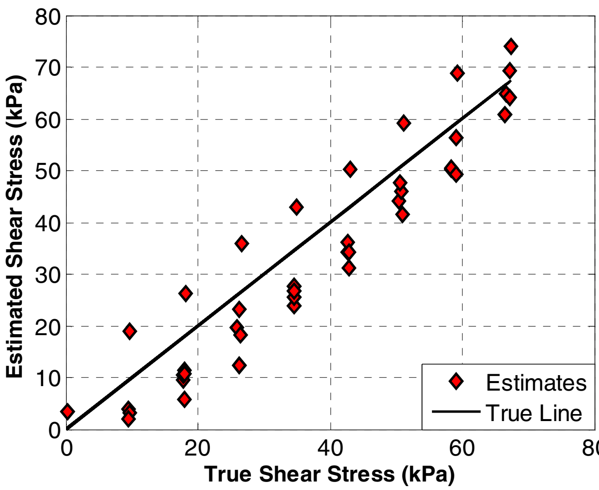

Figure 8. Shear stress can be estimated with an average accuracy of 89.45 %.

V. Conclusions and Future Work

We constructed and tested a sensor to simultaneously measure shear and normal stresses. The sensor was shown to be capable of isolating the cumulative effects of the normal and shear stresses with no significant crosstalk. Additionally, the applied stresses were estimated from the sensor output.

The relatively low accuracy in shear stress estimate can be attributed to the experimental noise in evaluating the sensitivity of the shear sensor (Figure 6) and its amplification in (6). When designing future versions of the sensor, this factor will be taken in to account while making sensitivity vs. area trade off decisions. Some of the error can also be attributed to a non-ruggedized test set up, which will also be addressed in the near future. To reduce the errors due to instantaneous spikes in sensor measurements, a finite response filter will be added to (6).

The next step in the development of this sensor will be to improve the sensitivity of the sensor to shear stress, and to build and test an array of these sensor cells. These will be challenging to achieve without increasing the dimensions of the sensor (thereby ruling out increasing electrode surface area for increased sensitivity), and adding a significantly larger number of electrical connections to measure the output of each sensor cell in the array.

References

[1] S. L. Lin, P. C. Tung, and N. E. Huang, "Data Analysis Using a Combination of Independent Component Analysis and Empirical Mode Decomposition," *Physical Review e*, vol. 79, no. 6, 2009.

[2] A. Nair, R. Hanspal, M. S. Zahedi, M. Saif, and K. Fisher, "Analyses of Prosthetic Episodes in Lower Limb Amputees," Prosthetics and Orthotics International, vol. 32, pp. 42-49, 2008.

[3] N. L. Dudek, M. B. Marks, and S. C. Marshall, "Skin Problems in Amputee Clinic," Am J Phys Med Rehabil, vol. 85, pp. 424-429, 5-2-0006.

[4] J. E. Sanders and C. H. Daly, "Measurement of Stresses in Three Orthogonal Directions at the Residual Limb-Prosthetic Socket Interface," *IEEE Transactions on Rehabilitation Engineering*, vol. 1, no. 2, pp. 79-85, 1993.

[5] J. E. Sanders, "Interface Mechanics in External Prosthetics: Review of Interface Stress Measurement Techniques," *Medical & Biological Engineering & Computing*, vol. 33, no. 4, pp. 509-516, 1995.

[6] J. E. Sanders, S. B. Mitchell, W. Yak-Nam, and K. Wu, "An Explant Model for the Investigation of Skin Adaptation to Mechanical Stress," *IEEE Transactions on Biomedical Engineering*, vol. 49, no. 12, pp. 1626-1631, 2002.

[7] J. C. Goh, P. V. Lee, and S. Y. Chong, "Compartive Study Between Patellar-Tendon-Bearing and Pressure Cast Prosthetic Sockets," J Rehabil Res Dev, vol. 41, pp. 491-501, 2004.

[8] J. E. Sanders, A. K. Jacobsen, and J. R. Fergason, "Effects of Fluid Insert Volume Changes on Socket Pressures and Shear Stresses: Case Studies from Two Trans-Tibial Amputee Subjects," Prosthetics and Orthotics International, vol. 30, pp. 257-269, 2006.

[9] T. L. Beil, G. M. Street, and S. J. Covey, "Interface Pressures During Ambulation Using Suction and Vacuum-Assisted Prosthetic Sockets," Journal of Rehabilitation Research and Development, vol. 41, pp. 693-700, 2002.

[10] T. L. Beil and G. M. Street, "Comparison of Interface Pressures with Pin and Suction Suspension Systems," Journal of Rehabilitation Research and Development, vol. 41, pp. 821-828, 2004.

[11] M. Zhang, A. R. Turner-Smith, V. C. Roberts, and A. Tanner, "Frictional Action at Lower Limb/Prosthetic Socket Interface," *Medical Engineering & Physics*, vol. 18, no. 3, pp. 207-214, Apr. 1996.

[12] J. E. Sanders, S. G. Zachariah, A. K. Jacobsen, and J. R. Fergason, "Changes in Interface Pressures and Shear Stresses Over Time on Trans-Tibial Amputee Subjects Ambulating With Prosthetic Limbs: Comparison of Diurnal and Six-Month Differences," *Journal of Biomechanics*, vol. 38, no. 8, pp. 1566-1573, 2005.

[13] K. Sundara-Rajan, G. I. Rowe, A. J. Simon, G. K. Klute, W. R. Ledoux, and A. V. Mamishev, "Shear Sensor for Lower Limb Prosthetic Applications," *2009 First Annual ORNL Biomedical Science & Engineering Conference*, Oak Ridge National Laboratory, Knoxville, TN, USA., 3-18-2009.

[14] K. Sundara-Rajan, G. I. Rowe, A. Bestick, A. V. Mamishev, G. K. Klute, and W. R. Ledoux, "Capacitive Sensing of Interfacial Forces in Prosthesis," 4-30-2010, pp. 73-76.

[15] J. Engel, J. Chen, C. Liu, B. R. Flachsbart, J. C. Selby, and M. A. Shannon, "Development of Polyimide-Based Flexible Tactile Sensing Skin," *Materials Research Society Symposium*, vol. 736, 2003, pp. D4.5.2-D4.5.6.

[16] M. H. Lee and H. R. Nicholls, "Review Article Tactile Sensing for Mechatronics--a State of the Art Survey," *Mechatronics*, vol. 9, no. 1, pp. 1-31, Feb. 1999.

[17] K. Hosokawa and R. Maeda, "In-Line Pressure Monitoring for Microfluidic Devices Using a Deformable Diffraction Grating," *14th IEEE International Conference on Micro Electro Mechanical Systems*, 2001, pp. 174-177.

[18] Y. Mo, Y. Okawa, M. Tajima, T. Nakai, N. Yoshiike, and K. Natukawa, "Micro-Machined Gas Sensor Array Based on Metal Film Micro-Heater," *Sensors and Actuators B: Chemical*, vol. 79, no. 2-3, pp. 175-181, Oct. 2001.

[19] H. Morimura, S. Shigematsu, and K. Machida, "A High-Resolution Capacitive Fingerprint Sensing Scheme With Charge-Transfer Technique and Automatic Contrast Emphasis," *Symposium on VLSI Circuits*, 1999, pp. 157-160.

[20] M. Sergio, N. Manaresi, M. Tartagni, R. Guerrieri, and R. Canegallo, "A Textile Based Capacitive Pressure Sensor," vol. 2, 2002, pp. 1625-1630.

[21] T. R. Filanc-Bowen, H. K. Geun, and Y. M. Shkel, "Novel Sensor Technology for Shear and Normal Strain Detection With Generalized Electrostriction," vol. 2, 2002, pp. 1648-1653.

[22] D. Johnston, Z. Ping, J. Hollerbach, and S. Jacobsen, "A Full Tactile Sensing Suite for Dextrous Robot Hands and Use in Contact Force Control," *Robotics and Automation, 1996. Proceedings., 1996 IEEE International Conference on*, vol. 4, 1996, pp. 3222-3227.